Determination of mask induced polarization effects on AltPSM mask structures

Ingo Höllein*, Silvio Teuber, Karsten Bubke
Advanced Mask Technology Center GmbH & Co. KG, Raehnitzer Allee 9, D-01109 Dresden, Germany

ABSTRACT

In the process of discussion of possible mask-types for the 5x nm node (half-pitch) and below, the alternating phase-shifting mask (AltPSM) is a potential candidate to be screened. The current scenario suggests using 193 nm immersion lithography with NA values of up to 1.2 and above. New optical effects from oblique incident angles, mask-induced polarization of the transmitted light and birefringence from the substrate need to be taken into account when the optical performance of a mask is evaluated. This paper addresses mask induced polarization effects from dense lines-and-space structures on a real mask. Measurements of the polarization dependent diffraction efficiencies have been performed on AltPSM masks. Experimental results show good agreement with simulations. A comparison with Binary Masks is made.

Keywords: AltPSM, Polarization, high NA, immersion, 50 nm lithography

1. MOTIVATION

Advanced mask types such as AltPSM are known since some years. This mask type proofed to have better imaging properties such as process window and a better mask error enhancement factor (MEEF) than the binary mask type. Their obvious benefit can only yield profit in production if certain mask properties like intensity and phase balance are controlled in an advanced way. Disadvantage of this mask type is the more complicated mask making process, which includes the high complexity of the mask design and the manufacturability. In order to decide about the mask scenario for a specific node, a trade-off between the imaging properties and the matters of mask making have to be made. In particular at small nodes, mask polarization is one effect influencing the imaging properties and shall therefore be investigated in order to have a more profound understanding of the AltPSM mask type.

2. INTRODUCTION into POLARIZATION EFFECTS

The resolution limit W of optical lithography is described by:

$$W = \frac{k_1 l}{NA} \tag{1}$$

where λ is the exposure wavelength, k_1 is a process factor and *NA* is the numerical aperture. NA is determined by the acceptance angle of the lens and the index of diffraction of the medium surrounding the lens:

$$NA = n \sin a \tag{2}$$

With water (n=1.47) as an immersion fluid, a NA of up to 1.2 and above is feasible resulting in a significantly better resolution.

According to the ITRS roadmap, one possible technology option for the 50 nm node is 193 nm immersion lithography. This would be the first node where the polarization effects become significant [1, 2].

* Phone: +49-351-4048-374, Fax: +49-351-4048-9374, E-mail: ingo.hoellein@amtc-dresden.com

Here the feature size on the mask (4 x 50 nm = 200nm) and the wavelength of 193 nm would be in the same range. As reported earlier, mask induced polarization effects become a concern when such small features interact with the light [2].

Reticle features with half pitches $\sim l$ act as a partial polarizer. In this case the transmission through the mask is polarization dependent, i.e. the diffraction spectrum for TE- and TM polarized light differs considerably from each other. The efficiency of the mask induced partial polarization is strongly influenced by the pitch, the line/pitch ratio, the absorber geometry and the absorber material.

As the interference of diffraction orders in the resist is substantially different for TE- and TM-components, the mask polarization behavior can have a considerable impact on the imaging properties of the overall system.

To quantitatively investigate the mask-induced polarization for relevant mask materials, a series of experiments and simulations were performed. The experimental setup is shown in Figure 1. An array of grating structures is illuminated with either TE-, TM- or unpolarized light and the efficiencies in the respective diffraction orders are detected with an angle resolved detector. As a figure of merit for mask polarization, the degree of polarization (DOP) is introduced:

$$DOP = \frac{I_{TE} - I_{TM}}{I_{TE} + I_{TM}}. \tag{3}$$

where I_{TE} and I_{TM} are the intensities diffracted in the respective orders. DOP of –100% indicates a fully TM polarized radiation, whereas +100% shows fully TE polarized radiation..

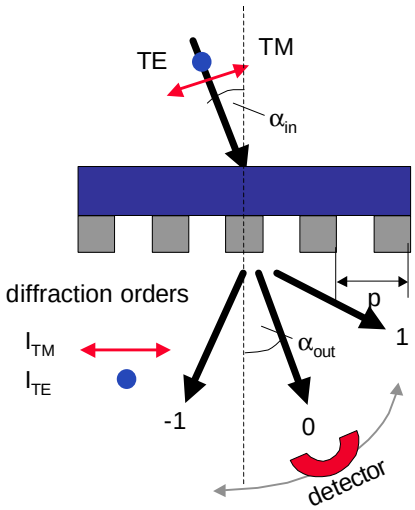

Figure 1 Schematics of the DoP evaluation set-up

3. AltPSM LITHOGRAPHY

First calculations show that the AltPSM mask type would meet the requirements for 50 nm half-pitch under immersion-settings [6]. The unit cell under investigation is shown in Figure 2.

Only the –1st and the 1st diffraction order are used for imaging. The design goal is to minimize the 0th diffraction order. This is achieved by the application of a portfolio of balancing methods, which are for example a) pattern biasing, b) quartz undercut and c) adjusting the quartz etch-depth.

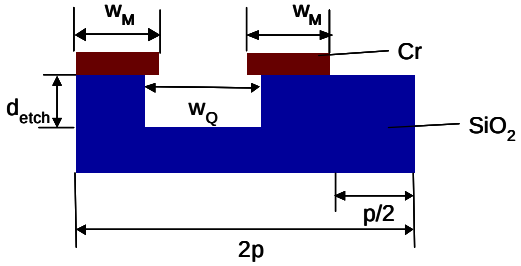

Figure 2 Structure of unit cell for an AltPSM mask with p: pitch, d_{etch}: etch depth, w_M : width of chrome absorber, w_Q: width of quartz trench

In all simulations a mask with an exact Pi-phase shift in the respective structure is assumed. Further, the mask is simplified in the way $w_m = w_Q = p/2$ and does therefore not take into account the balancing methods.

4. MASK DESIGN, FABRICATION and EXPERIMENTAL SETUP

The investigations described in this paper are based on three pillars:

I. AltPSM Test mask

The AltPSM mask was patterned at the AMTC using the standard process for the 90nm ground rule. The mask design consists of fields with an area of 4mmx4mm containing lines and spaces with a specified pitch size and duty cycle. The fields are separated by a distance of 1mm and arranged in a matrix with different fields corresponding to different pitches and line/pitch ratios. The mask pitch ranges from 1200nm to 300nm. The same layout was used for earlier DoP experiments recently published by AMTC [1, 5].

The mask manufacturing consists of two parts. At first the grating structures were patterned into the chromium layer. The resulting grating structures were characterized with a CD-SEM as well as with a surface-nanoprofiler (SNP). With those measurement techniques the Cr-structures can be well characterized with respect to line width, line/space ratio, space width as well as sidewall angle. All structures were well controlled with respect to mask pitch and sidewall angle. In this polarization study transmission measurements on structures with a line/pitch ratio of 0.5 were performed.

In a second step, the quartz step was applied. As mentioned in section 3, the mask structures must be balanced in order to reach the best lithographic performance. Therefore the phase and transmission of the clear fields must be controlled. For the mask under investigation, the balancing methods undercut and etch-depth adjustment were applied. Due to reactive ion etching (RIE) lag, etch depth uniformity and different clear and pitch sizes, the balancing could be only optimized for one target structure. Since we used an optimized process for 90nm ground rule structures, most of the structures of interest were not in balancing specification. Printing these features, both an offset and slope error will occur. The offset defines the transmission difference between 0- and Pi-shifting regions on the mask and the slope defines the phase error between these two regions. The structures of interest were characterized with both AIMS^{TM} and SNP measurements down to the resolution limit of the measurement tools. A deviation from optimum balancing was observed. Figure 3 shows as an example the resulting offset behavior as a function of pitch. This curve is derived from the AIMS measurements. The offset increases with decreasing mask pitch. This shows, that for smaller structures the transmission difference between 0- and Pi-shifting regions needs to be adjusted, i.e., by adapting the undercut. In figure 4 the trench depth variation as a function of the mask pitch is depicted. The deviation from the constant curve is caused by the RIE lag. However, over the whole measured pitch range only slight trench depth variation was observed. As a consequence the phase shifting region was not a perfect Pi-shifter over the whole pitch range.

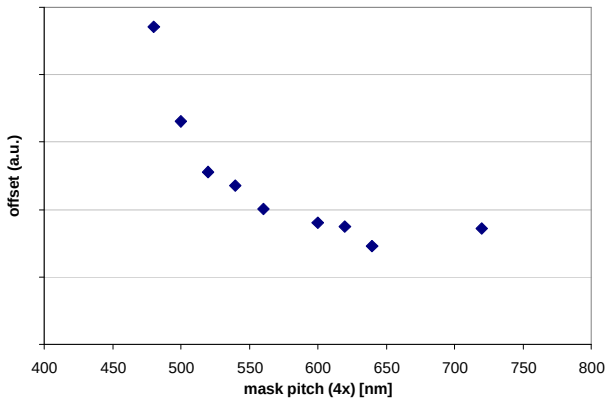

Figure 3 Measured CD offset deviation due to transmission imbalancing of the clear mask structures derived from AIMS measurements.

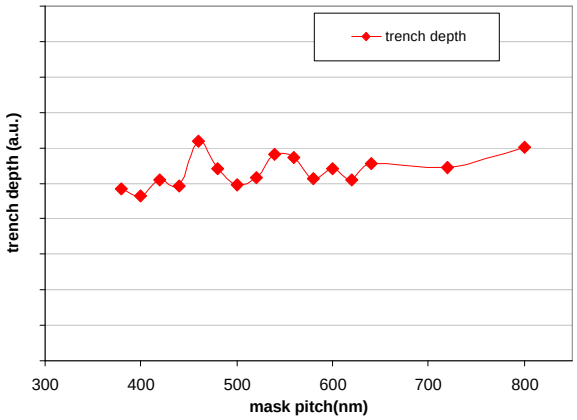

Figure 4 Measured trench depth of Pi-phase-shifting region as a function of the mask pitch.

II. Experimental set-up

The polarization measurements were performed at the Fraunhofer Institute (IOF) in Jena using a VUV photospectrometer [2, 3]. The measurement system uses a deuterium lamp as light source, a grating monochromator in order to select a specified wavelength, a Rochom prism of MgF2 as UV-polarizer, a sample holder and a photo multiplier. Angle resolved transmission measurements were performed at 193.4nm at different polarization directions. The mask patterns were illuminated from the backside. The obtained angle resolved transmission spectra were analyzed with respect to the intensities of the 0^{th} and the -1^{st} diffraction order. A Gaussian-like pulse shape is fitted to the diffraction order peaks in order to get the angle position and the maximum intensity.

III. Simulations

All DoP calculations shown on the next pages were performed using G-Solver Software[4]. The simulations for the AltPSM refers to a mask with a perfect Pi-phase-shift in the respective structure.

The manufacturing and balancing constraints and the test masks´ deviations from the perfect-mask-structure indicate, that only a qualitative comparison between experiment and simulation is possible.

5. SIMULATION and MEASUREMENT RESULTS of AltPSM MASK STRUCTURES

5.1. Transmission of the AltPSM mask at perpendicular incidence: Comparison of experimental data and simulation

Figure 5 and Figure 6 show the normalized transmission for TE and TM measured behind the mask using the experimental set-up described in the last section. The mask-pitch refers to the measured pitch derived from the SNP and SEM measurements. Measurements were performed on mask pitches from 1600nm down to 300nm. The line/pitch ratio of all investigated structures was 0.5.

Comparing the absolute magnitude of the normalized transmission in the 0^{th} and the 1^{st} diffraction order, it becomes obvious that the transmission of the 0^{th} order is about one order of magnitude smaller than the transmission of the 1^{st} order. This is in-line with the design goal of minimizing the 0^{th} diffraction order. The real mask shows even less transmission than the simulated ideal mask. This can be explained with the mentioned simplification of the simulation, which is not taking into account the applied balancing methods. Another cause for deviations between the simulated

curves and the measurement results are inaccurate n and k model assumptions used in the simulation. Nevertheless, the transmission of the 1st diffraction order shows good agreement between simulation and measurement.

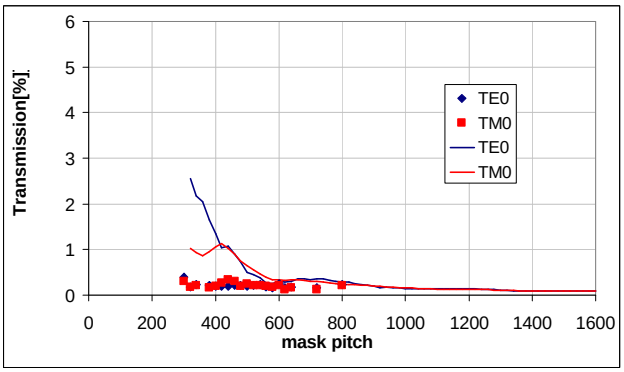

Figure 5 Normalized transmission of the 0th diffraction order of illuminated dense lines /space gratings with fixed duty cycle (line/pitch=0.5) and varying pitch size under normal incidence illumination: comparison between measurement (squares) and simulation (line).

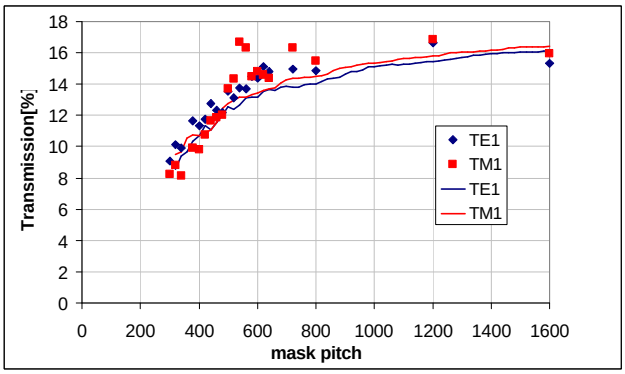

Figure 6 Normalized transmission of the 1st diffraction order of illuminated dense lines /space gratings with fixed duty cycle (line/pitch=0.5) and varying pitch size under normal incidence illumination: comparison between measurement (squares) and simulation (line).

5.2. The Degree of Polarization DoP1 of AltPSM grating structures for different pitches

Using equation (3) and the transmission data depicted in Figure 6, the DoP1 can be calculated as shown in Figure 7. The squares represent the measurement results from the diffraction experiment. The solid curves represent the simulation. The DoP0 is not discussed here because the 0th order would not be used for imaging AltPSM grating structures.

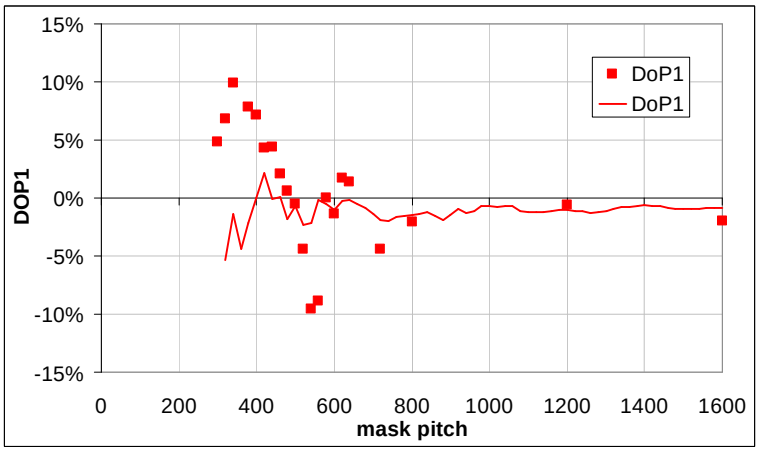

Figure 7 Degree of polarization (DoP) of the 1st diffraction order of illuminated dense lines /space gratings with fixed duty cycle (line/pitch=0.5) and varying pitch size under normal incidence illumination: comparison between measurement (squares) and simulation (line).

The measurement results show small polarization effects for all investigated pitches. In the mask pitch range between 450 and 600 nm (corresponding to the 75 to 55nm half-pitch range on wafer level), the AltPSM grating structure shows partial TM polarization with a maximum value of –10% at a mask pitch of approx. 500 nm. From 400nm downwards, TE polarization dominates with a maximum value of +10% at a mask pitch of approx. 350nm.

For larger pitches, experiment and simulation are in good agreement. From 400nm downwards, the deviations become more significant. This can be explained with the non-balanced simulated mask as already discussed in section 5.1.

It should be highlighted here that the smallest experimentally explored grating structure of 300 nm (corresponding to the 38 nm node half pitch) shows no

increased polarization behavior. Altogether, the investigated AltPSM grating structures show very little polarization effects.

6. INFLUENCE of DIFFERENT BALANCING METHODS on the DOP1

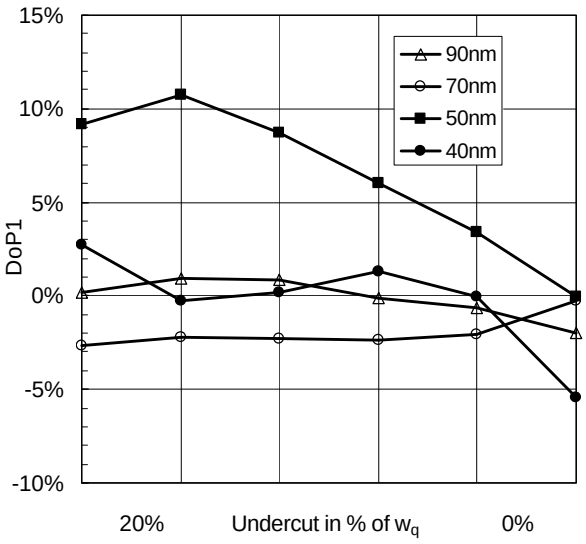

Figure 8 Simulated DoP1 of AltPSM grating structures for different pitches as a function of the undercut size

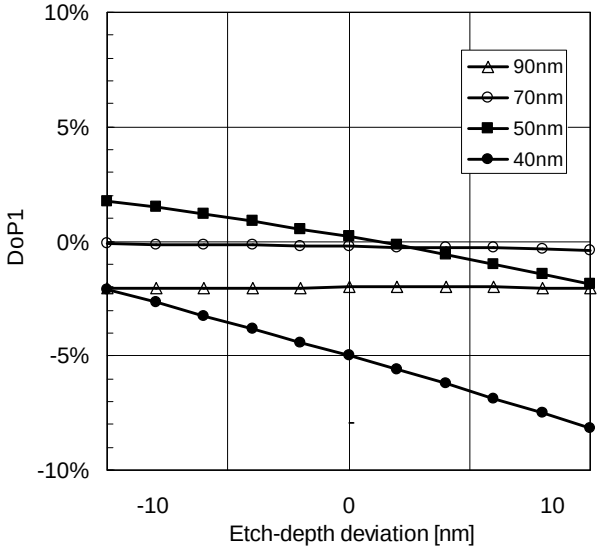

Figure 9 Simulated DoP1 of AltPSM grating structures for different pitches as a function of the deviation of the etch-depth of the ideal Pi-phase shifting etch depth

In order to determine the DoP sensitivity of the AltPSM balancing methods, two balancing parameters undercut and etch-depths have been investigated via simulation.

Figure 8 depicts the DoP1 variation as a function of the undercut size ratio for a fixed w_m=p/2 (see Figure 2). In the case w_q= w_m = p/2 (right edge of Figure 8) no under-etch was applied. No clear correlation between mask pitch, undercut size and DOP1 can be observed. Interestingly the 50nm structures show more polarization effects than the 40nm structures. The 50nm structures show increasing polarization effects in TE with an increasing undercut size. A maximum value of 9% has been calculated for an undercut of 20% w_q.

Figure 9 depicts the DoP1 variation as a function of the etch-depth. The 0 etch-depth deviation point represents the ideal etch-depth corresponding to a Pi-phase shift. The DoP1 sensitivity slightly increases from approx. 0 for 90 nm structures to approx. 4% for 50 nm structures. A significant jump to 8% can be observed for the 40 nm structures.

Adding up the impact of undercut and etch-depth variation to the DOP1 as depicted in Figure 7, the magnitude of the deviation between the simulation and the experiment can be explained.

7. COMPARISON of ALTPSM and CoG STRUCTURES

The AMTC reported earlier on diffraction experiments performed on chrome-on-glass masks (CoG) [1]. The mask material, the mask layout and the experimental set-up are the same as for the AltPSM set-up of this investigation. Technically the only difference between the CoG and the AltPSM mask is the quartz etch step, which creates a Pi-phase shifting region at every second space. For both mask types the 1st diffraction order is relevant for imaging.

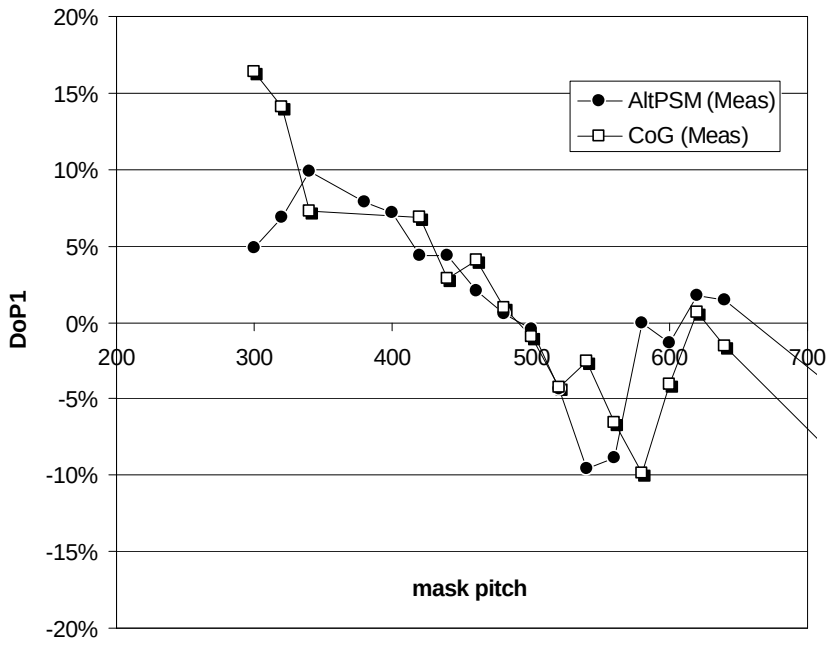

By a comparison of the measured DoP1 data of the CoG and the AltPSM mask, the impact of this quartz-etch-step can be quantified. Figure 10 shows the measured DoP1 for AltPSM and binary mask structures. For mask pitches down to approx. 350 nm both curves are nearly identical. For structures below 350 nm the curves significantly deviate. Whereas the AltPSM DoP1 decreases from approx. 10% for 350 nm structures to 5% for 300 nm structures, the DoP1 of the CoG mask increases from 7% to over 15% in the same region. It can be stated, that the quartz-etch reduces the DoP1 for small pitches.

Figure 10 Comparison of the measured DoP1 for CoG and AltPSM grating structures

8. SUMMARY

In this paper the polarization effects of AltPSM masks have been discussed. Diffraction experiments have been performed on a test mask with grating structures with a pitch range from 1600nm to 300nm. In addition rigorous simulations were performed and compared with the experiment. Experiment and simulation are in good qualitative agreement. The AltPSM mask shows small polarization effect even for the smallest explored pitches, which correspond to the 38 nm node half-pitch (wafer level).

In a second step, the sensitivity of two different AltPSM balancing methods in regards to the DoP1 has been investigated via simulation. The impact of undercut and etch-depth variation on the DoP1 is considerably low for structures down to 40 nm half-pitch (wafer level) independent of the undercut size. An exception are the 50nm structures, which increase linear in DoP1 with increasing undercut.

In a third step, a comparison of the AltPSM with a CoG mask has been made in order to derive the impact of the quartz-etch step on the DoP1: The quartz-etch decreases the polarization effect in the first diffraction order for small structures.

The formation of the resist image on the wafer is a complex process with many interdependent parameters. Therefore it is not possible to make a conclusion on the suitability of a specific mask type for 50 nm hp lithography based solely on its polarization properties [7]. Nevertheless, with respect to polarization effects, AltPSM masks seem to have a potential for even sub 45 nm lithography.

ACKNOWLEDGEMENTS

AMTC is a joint venture of Infineon, AMD and DuPont Photomasks and gratefully acknowledges the financial support by the German Federal Ministry of Education and Research (BMBF) under Contract No. 01M3154A ("Abbildungsmethodiken für nanoelektronische Bauelemente")

The authors would like to thank the Fraunhofer Institute IOF in Jena for their measurement capability and also for a lot of fruitful discussions.

REFERENCES

1. Silvio Teuber, Kartsen Bubke, Ingo Höllein, *Determination of mask induced polarization effects occurring in Hyper NA immersion lithography* in SPIE 2005
2. Estroff, Y. Fan, A. Bourov, F. Cropanese, N. Lafferty, L. Zavyalova and B. Smith, *Mask induced Polarization*, SPIE2004
3. J. Heber, A. Gatto, N. Kaiser, *Spectrophotometry in the vacuum UV*, Boulder 2002
4. Web site reference: *http://www.gsolver.com/*
5. K. Bubke, S. Teuber, I. Hoellein, H. Becker, H. Seitz, U. Buttgereit, *Investigation of Polarization Effects on new Mask Materials*, t.b.p. in SPIE 2005
6. B.J. Lin, Plenary Speech at SPIE, SPIE Proc. Vol. 4688, p.11, 2002
7. Donis G. Flagello, Steve Hansen, Bernd Geh, Michael Totzeck, *Challenges with Hyper NA (NA>1) Polarization light Lithography for Sub l/4 resolution* in SPIE2005